Effect of Rotational Speed on Axial Force and Spindle Torque during FSSW of AA6063/HE9 and CRCA/IS-513 steel with a Consumable Sheet

WCMNM 2020

Sukanta Das[1] R. Ganesh Narayanan[2]

[1] *Department of Mechanical Engineering, Indian Institute of Technology Guwahati, Guwahati, India*
[2] *Department of Mechanical Engineering , Indian Institute of Technology Guwahati, Guwahati, India*

Abstract

Joining Aluminum to steel sheets has always been a challenging task. Fusion welding processes had not been found advantageous in joining the materials. However, the fabrication of aluminum to steel joints has significant prospects in the automotive industry. In the present work, Friction Stir Spot Welding (FSSW) has been used to join these two dissimilar aluminum and steel sheets in butt configuration with an Aluminum consumable sheet contacting the FSSW tool. The consumable sheet is placed above the Steel-Aluminum pair. In this way, the tool has no contact with the steel sheet during joint formation. The current work investigates the effect of the tool rotational speed on the z-direction axial force and spindle torque. Five different rotational speeds are used to understand the influence. The outcomes of the work can be extended to micro joining for assembling micro parts.

Keywords: Fusion welding, FSSW, FSW, rotational speed, force, spindle torque.

1. Introduction

Friction Stir Spot welding (FSSW) is a solid-state joining process and a variant of the friction stir welding process [1]. This process is invented by Mazda [2]. FSSW process starts with the plunging operation in which the tool is plunged into the base sheets. During stirring, the rotational tool rotates in the same vertical position for a set dwell time to generate proper frictional heat (Fig. 1). The frictional heat softens and plasticized the material, resulting in the proper material flow. After achieving the plasticized state during dwelling, the tool is retracted, leaving a keyhole [3].

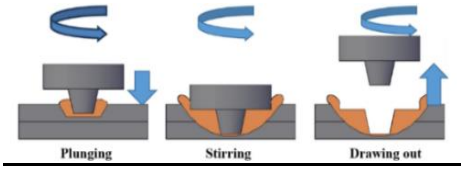

Fig. 1. Schematic of FSSW (with permission from Mubiayi et al., (2018), Copyright Elsevier)

Joining Aluminium to Steel is one of the prominent needs to reduce the structures total weight in the automotive industry. However, solidification defects, hydrogen embrittlement, and intermetallic compound formation are the common shortcomings when fusion welding processes are used for joining these two dissimilar alloys.

Solid-state welding processes like FSSW is an alternative to avoid such defects. However, tool wear occurs during FSSW. Many researchers have used tool offset, meaning offsetting the tool towards the softer material. In this case, a decrease in joint tensile strength is witnessed. Materials like PCBN and refractory materials are commonly used materials to fabricate the tool [4]. Due to the high ductile-to-brittle transition temperatures of the material, they undergo deformation and fracture. Preheating is another way to reduce tool wear. An increase in intragranular corrosion during preheating of austenitic stainless steel, embrittlement developed during preheating of precipitation-hardened steels, and ferrite steels are some limitations associated with preheating [5].

2. FSSW of dissimilar sheets with a consumable

2.1. Methodology

With respect to the problems mentioned above, a new method of joining Aluminum to Steel sheets has been introduced in this work. In this, the rotating tool will have no contact with the base sheets to be joined. Instead, it touches the consumable Aluminum sheet, which is kept above the base sheets to be joined (Fig. 2). Due to such an arrangement, tool wear can be avoided. While doing so, the joint properties will be significantly modified. In this context, the main aim of the present work is to address the effect of rotation speed on the tool axial force and torque during the joining process.

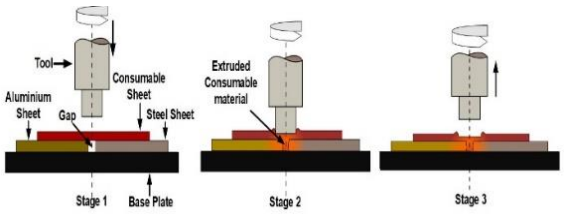

Fig. 2. Schematic of FSSW of dissimilar aluminum and steel alloy with a consumable sheet.

As shown in Fig. 2, the base sheets (aluminum and steel) to be joined are located, maintaining a specific gap between each other. In this work, a pinless flat cylindrical tool is used. Pinless tools ensure

the heat is uniformly produced for a reasonable amount of time over the top surface [6]. The pinless tool eliminates the keyhole, which will always be present at the end of the process. Keyhole acts as stress concentration and imparts lower strength to the joints [7].

After the base sheets and the consumable sheet are properly clamped, the process starts with plunging the tool into the consumable sheet and then the base sheets. As the tool progresses downward, severe forging pressure and frictional heat are generated at the interface, due to which the softened consumable gets plasticized and extruded through the gap. Later, it is welded with the base sheets. The rotating tool will never contact the faying surfaces to be joined in this processing technique, eliminating the tool wear.

This study will discuss the effect of tool rotational speed on two output parameters, i.e., axial force in z-direction and spindle torque. Fig. 3 shows the torque and force sensors along with the data logger. The sensor is present at the bottom of the base plate, and a data logger is connected to store and transfer the data.

(a) (b)

Fig. 3. (a) Force and Torque sensor (b) Data acquisition

2.2. Material characteristics

Tensile tests were conducted on the base sheets as per ASTM E8 standard in a universal testing machine (INSTRON, Model 8801) at a cross-head speed of 1 mm/min to obtain load-displacement data. Engineering stress-strain data were evaluated as per the usual procedure (Fig. 4). The plastic strain ratio (R-value) of the base sheets is also measured following ASTM E517-19 standards (Table 1).

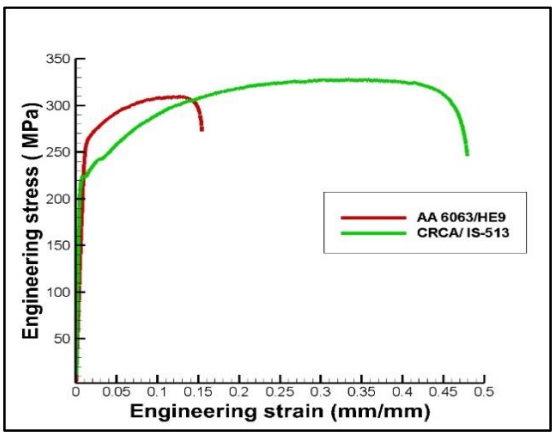

Fig. 4. Stress-strain behavior of AA 6063 and CRCA IS-513 grade sheets

Table 1
R-value of base materials

Material	Rolling direction	Plastic strain ratio
AA6063/HE9	0°	0.59
	45°	0.67
	90°	0.80
CRCA/ IS-513	0°	0.69
	45°	0.81
	90°	0.97

The chemical composition (weight in %) of the base materials is shown in Table 2 and Table 3. The composition has been found out by the wet method (IS-504-2002).

Table 2
Chemical composition of AA6063/HE9

Material	Si %	Cu %	Mn %	Fe %	Mg %	Zn %	Al %
AA6063/ HE9	0.6	0.09	0.09	0.4	0.44	0.04	Bal

Table 3
Chemical composition of CRCA/IS-513 steel

Material	C %	Si %	Mn %	S %	P %	Fe %
CRCA/ IS- 513	0.1	0.24	0.58	0.016	0.018	Bal

3. Experimental details

AA6063/HE9 and low carbon CRCA/IS-513 steel is used as base sheet material. The dimension of the base sheets is 105 mm× 45 mm× 1.5 mm. The consumable sheet is the same as the aluminum base sheet material of dimension 75 mm × 45 mm × 1.5 mm. After cutting the samples, the edges were polished with 320 grit size emery paper and adequately cleaned with acetone. Fig. 5 shows the arrangement of the base materials along with the consumable sheet. A gap of 1.5 mm is maintained in every experiment conducted.

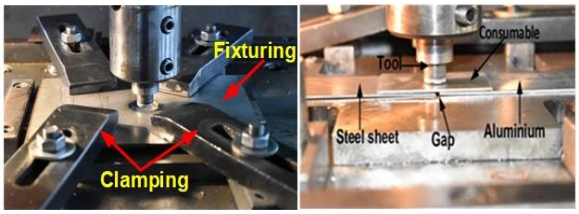

(a) (b)

Fig. 5. (a) Experimental setup (b) Arrangement of sheets

As shown in Fig. 5, a pinless tool is used in the experiments which has been fabricated from H13 tool steel. It has a shoulder of 15 mm diameter and 12 mm height. All the experiments are performed with a constant plunge speed of 2 mm/min, constant plunge depth of 2 mm and a constant dwell time of 5 sec and varying tool rotational speeds.

Fig. 6. Tool used in experiments

4. Results and discussion

In this section, all the results of the experiments are discussed. The rotation speed is varied at 233, 360, 612, 900, and 1200 rpm, as these are available levels in the machine. Table 4 depicts the welded specimen welded at a different rotational speed of the tool.

Table 4
Welded specimens at various rotational speeds

233 rpm	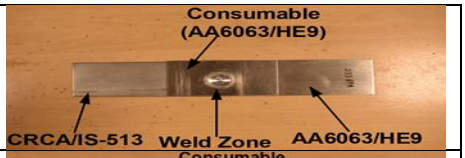
360 rpm	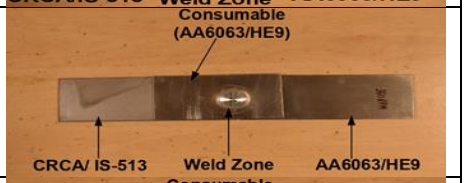
612 rpm	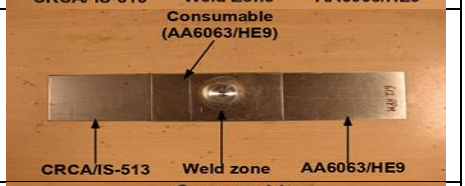
900 rpm	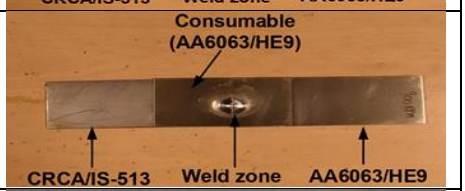
1200 rpm	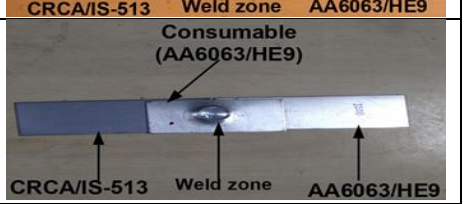

The experiment starts with 233 rpm, which is the lowest rotational speed on the machine. As shown in Figure. 7, the total duration of the spot welding is 65 sec, which means the entire plunging stage is of 60 sec followed by 5 sec dwell time. The lower rotational speed (233 rpm) is characterized by higher axial force and spindle torque. The maximum axial force and spindle torque of all the cases has been provided in Table 5.

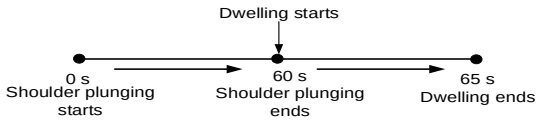

Fig. 7. Total duration of the process

Table 5

Maximum axial force and spindle torque recorded during the experiments

Rotational speed (RPM)	Maximum axial force (N)	Maximum spindle torque (N-mm)
233	2911	533
360	1124	215
612	1083	208
900	1046	184
1200	943	150

The axial force and torque trends for 233 rpm are somewhat different from the other five rotational speeds. Fig. 8 and Fig. 9 show an initial sudden peak in the axial force and torque in the case of 233 rpm. As the tool progresses, the tool meets cold consumable aluminum material. Due to lower rotational speed, the temperature generated is not enough to deform the consumable material, which leads to an increase in axial force and spindle torque. After the sudden peak, a sudden drop is observed in force and torque. This sudden drop can be explained as adhesion of aluminum to the tool shoulder leading to the decrease in coefficient of friction, and hence decrease in force and torque.

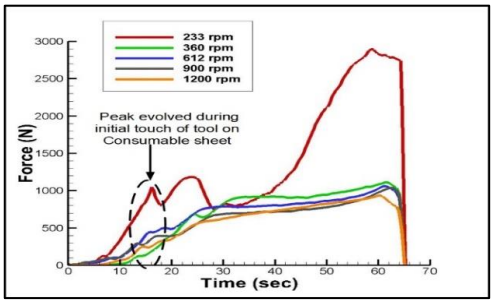

Fig. 8. Axial force recorded for different experiments

The second peak after the sudden drop follows an increase in force and torque again. Every time the tool progresses more into the consumable sheet, it meets fresh undeformed aluminum material. Due to the lower rotational speed, the heat generated is not enough to soften and plasticize the consumable material, leading

to increased axial force and spindle torque. The trend matches with the work of Bakavos et al. [8] for conventional FSSW with a pinless tool. For the 233 rpm, when the tool is plunged around half away into the consumable sheet, a gradually increasing trend followed in the force and torque. This type of trend can be explained by the fact that when the tool tries to force the upcoming extruded material downward, the tool experiences a significant rise in force and torque. Suryanarayanan and Sridhar [9] explained this trend for joining two aluminum alloys with a pinless tool by the conventional FSSW process.

Unlike 233 rpm, the trend of force and torque for other rotational speeds is not that peculiar. From the start of the plunging to the end of the plunging, a gradual increase in trend is observed, followed by the sudden drop when the tool is retracted fully from the joint.

Fig. 8. and Fig. 9 also revealed a decrease in the axial force and spindle torque with the increase in rotational speed from 233 rpm to 1200 rpm. High rotational speeds employ heavy stirring, due to which a massive amount of heat is generated at the tool-consumable interface. This induced heat allows the tool to take less axial force and torque to deform and plasticized the consumable material. The trend matches with the work of Zimmer et al. [10] during the plunging stage of the FSW process.

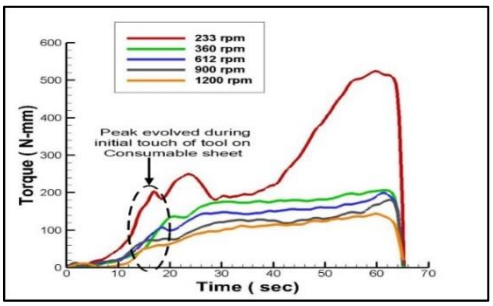

Fig. 9. Spindle torque recorded for different experiments

For each of the experiments conducted, the peak axial force and spindle torque occurred at the end of the plunging stage. At the dwelling stage, it has been seen that a gradual decrease is observed for both the output parameters, followed by a sudden drop. Sudden drop signifies full retraction of the rotating tool after the completion of the dwelling time.

4. Conclusions

A novel FSSW process has been introduced in which a consumable sheet is used to join two dissimilar grade sheets. The tool has no contact with the sheets to be joined, minimizing the wear and tear of the tool. The rotational tool speed heavily influences axial force and spindle torque. The highest rotational speed (1200 rpm) requires less force and torque than the lowest rotational speed (233 rpm). The main reason behind this is that the higher rotation speed leads to higher process temperature, making the material soft easily, requiring less torque and force for joint formation. At 233 rpm, during plunging, the tool required more force and torque to deform the consumable material. The highest axial force and spindle torque occur at the end of the plunging stage. There is a decrease in force and torque during dwell time followed by a sudden drop due to tool retraction.

Acknowledgment

The authors are grateful to the Mechanical Engineering department's central workshop, IIT Guwahati, for job preparation, tool fabrication, and carrying out all the experiments.

References

[1] M. Fujimoto et al., "Development of Friction Spot Joining," Weld. World, Mar. 2005; vol. 49, no. 3–4, pp. 18–21.

[2] R. S. Mishra et al., "Friction stir welding and processing," Mater. Sci. Eng. R Rep., Aug. 2005; vol. 50, no. 1–2, pp. 1–78.

[3] M. P. Mubiayi et al., "Current state of friction stir spot welding between aluminium and copper," Mater. Today Proc., 2018; vol. 5, no. 9, pp. 18633–18640.

[4] F. C. Liu et al., "A review of friction stir welding of steels: Tool, material flow, microstructure, and properties," J. Mater. Sci. Technol., Jan. 2018; vol. 34, no. 1, pp. 39–57.

[5] H. Bang et al., "Gas tungsten arc welding assisted hybrid friction stir welding of dissimilar materials Al6061-T6 aluminum alloy and STS304 stainless steel," Mater. Des., May 2012; vol. 37, pp. 48–55.

[6] S. R. Yazdi et al., "Pinless tool for FSSW of AA 6061-T6 aluminum alloy," J. Mater. Process. Technol., May 2019; vol. 267, pp. 44–51.

[7] K. P. Mehta et al., "On FSW Keyhole Removal to Improve Volume Defect Using Pin Less Tool," Key Eng. Mater., Sep. 2019; vol. 821, pp. 215–221.

[8] D. Bakavos et al., "Effect of reduced or zero pin length and anvil insulation on friction stir spot welding thin gauge 6111 automotive sheet," Sci. Technol. Weld. Join., Jul. 2009; vol. 14, no. 5, pp. 443–456.

[9] R. Suryanarayanan et al., "Effect of Process Parameters in Pinless Friction Stir Spot Welding of Al 5754-Al 6061 Alloys," Metallogr. Microstruct. Anal., Apr. 2020; vol. 9, no. 2, pp. 261–272.

[10] S. Zimmer et al., "Experimental investigation of the influence of the FSW plunge processing parameters on the maximum generated force and torque," Int. J. Adv. Manuf. Technol., Mar. 2010; vol. 47, no. 1–4, pp. 201–215.